Proc. Natl. Acad. Sci. USA
Vol. 93, pp. 8934–8939, August 1996
Biochemistry

Molecular characterization of the mosquito vitellogenin receptor reveals unexpected high homology to the *Drosophila* yolk protein receptor

(*Aedes aegypti*/vitellogenesis/receptor-mediated endocytosis/egg development/low density lipoprotein receptor)

THOMAS W. SAPPINGTON*, VLADIMIR A. KOKOZA*, WEN-LONG CHO†, AND ALEXANDER S. RAIKHEL*‡

*Department of Entomology and Programs in Genetics and Cell and Molecular Biology, Michigan State University, East Lansing, MI 48824; and †Department of Parasitology, National Yang-Ming University, Shih-pai, Taipei 112, Taiwan, Republic of China

Communicated by John H. Law, The University of Arizona, Tucson, AZ, May 17, 1996 (received for review February 26, 1996)

ABSTRACT **The mosquito (*Aedes aegypti*) vitellogenin receptor (*Aa*VgR) is a large membrane-bound protein (214 kDa when linearized) that mediates internalization of vitellogenin, the major yolk-protein precursor, by oocytes during egg development. We have cloned and sequenced two cDNA fragments encompassing the entire coding region of *Aa*VgR mRNA, to our knowledge the first insect VgR sequence to be reported. The 7.3-kb *Aa*VgR mRNA is present only in female germ-line cells and is abundant in previtellogenic oocytes, suggesting that the *Aa*VgR gene is expressed early in oocyte differentiation. The deduced amino acid sequence predicts a 202.7-kDa protein before posttranslational processing. The *Aa*VgR is a member of the low density lipoprotein receptor superfamily, sharing significant homology with the chicken (*Gallus gallus*) VgR and particularly the *Drosophila melanogaster* yolk protein receptor, in spite of a very different ligand for the latter. Distance-based phylogenetic analyses suggest that the insect VgR/yolk protein receptor lineage and the vertebrate VgR/low density lipoprotein receptor lineage diverged before the bifurcation of nematode and deuterostome lines.**

The developing embryo of an oviparous animal draws practically all of its requisite nutrients from a cache of proteins, lipids, and carbohydrates stored within the egg as yolk. Yolk-protein precursors are synthesized extraovarially and transported to the developing egg where they are specifically recognized and bound by membrane-spanning cell-surface receptors. Receptor–ligand complexes accumulate in clathrin-coated pits, which pinch-off into the cytoplasm, a fundamental process ubiquitous among cells for internalizing macromolecules referred to as receptor-mediated endocytosis (1, 2). The insect oocyte provides an excellent system for studying receptor-mediated endocytosis because of the high intensity of protein uptake. Mosquitoes are especially useful models in this regard, because a tightly regulated series of physiological events associated with egg maturation is synchronized across all primary oocytes by a blood meal.

In the yellow fever mosquito *Aedes aegypti* (*Aa*), oocyte size increases more than 300-fold within 36 h of a blood meal (3), largely through the specific accumulation of the major yolk-protein precursor vitellogenin (*Aa*Vg). This impressive biological feat depends on the proper interaction of *Aa*Vg with its receptor (*Aa*VgR) on the oocyte surface. In addition to its exceptional value as a model for studying receptor-mediated endocytosis, this system is also a promising target for future novel control strategies. For example, interruption of the receptor–ligand interaction would block egg development, and the *Aa*VgR could serve as a target for an antimosquito vaccine (4). A prerequisite to successful manipulation of this system is a thorough understanding of the proteins involved: their structures, interactions, regulation, and expression. Meaningful progress on all of these fronts hinges on knowledge of the primary structures of both *Aa*Vg, which we recently determined (5), and *Aa*VgR.

Significant advances in our understanding of Vgs, VgRs, and their interactions have been made over the last 15–20 years (for reviews, see refs. 6–8). The sequences of several vertebrate and invertebrate Vgs are known. They are large (200–700 kDa) homologous phospholipoglycoproteins that serve as the principal yolk-protein precursor in the nematode, most insects, and vertebrates (5, 6, 9, 10). To our knowledge, the only previously reported sequence of a VgR (11) is that of the chicken (*Gallus gallus*) (*Gg*), a 95-kDa receptor (*Gg*VgR/LR8) that internalizes *Gg*Vg and at least three other components of chicken yolk (12, 13). Higher Diptera such as *Drosophila* synthesize relatively small (44–51 kDa) yolk-protein precursors (by convention designated YPs) homologous to lipoprotein lipases (10, 14), rather than the large Vgs found in other insects. Though sometimes referred to as "vitellogenins" in a broad sense, and although the protein coded by the yolkless gene in *Drosophila melanogaster* has been called a "vitellogenin receptor" (15), YPs are not homologous to the Vgs of other organisms (14). Thus, we will follow conventional terminology, which distinguishes between these unrelated classes of protein. Taking advantage of the powerful genetic tools available for work with *Drosophila*, the cDNA of the yolkless gene in *D. melanogaster* encoding the putative YP receptor (*Dm*YPR) was recently sequenced (15). However, such genetic tools are currently unavailable for other insects. Consequently, determining the molecular nature of an insect VgR (*ins*VgR) has been, until now, an intractable problem because of the difficulties inherent in performing the requisite preliminary biochemical manipulations of low-abundance proteins from small organisms.

*Ins*VgRs are large (180–214 kDa) molecules, roughly twice the size of vertebrate VgRs (95–115 kDa) (7, 8, 16). Binding kinetics studies have shown that *ins*Vgs have very high affinities to follicle/ovary membrane preparations (K_d = 13–200 nM) and to solubilized or purified *ins*VgRs (K_d = 15–42 nM) (6, 16, 17). More is known about the biochemical and molecular properties of the *Aa*VgR than that of any other inverte-

The publication costs of this article were defrayed in part by page charge payment. This article must therefore be hereby marked "*advertisement*" in accordance with 18 U.S.C. §1734 solely to indicate this fact.

Abbreviations: Vg, vitellogenin; VgR, vitellogen receptor; YP, yolk protein; YPR, yolk protein receptor; LDLR, low density lipoprotein receptor; LR8, LDLR relative with eight binding repeats; *Aa*, *Aedes aegypti*; *Dm*, *Drosophila melanogaster*; *Gg*, *Gallus gallus*; *ins*, insect; LRP, LDLR-related protein.

Data deposition: The sequence reported in this paper has been deposited in the GenBank data base [accession no. L77800 (for the nucleotide sequence of the coding region of the *Aedes aegypti* vitellogenin receptor)].

‡To whom reprint requests should be addressed at: Department of Entomology, S-136 Plant Biology Building, Michigan State University, East Lansing, MI 48824. e-mail: araikhel@ibm.cl.msu.edu.

brate. Ligand blotting identified it as a 205-kDa protein under nonreducing conditions (18), and native gel analysis indicated that it probably occurs as a noncovalent homodimer (17). Immunoprecipitation experiments demonstrated that the *Aa*VgR does not consist of smaller subunits and that it has an apparent molecular mass of 214 kDa when internal disulfide bonds are reduced (17).

Purification and subsequent microsequencing of tryptic fragments of the *Aa*VgR protein (17) has permitted rapid progress in its molecular characterization. The entire coding region of its mRNA transcript has been sequenced, the first *ins*VgR for which this has been accomplished. We report herein the results of sequence analyses, *Aa*VgR mRNA cellular distribution experiments, and phylogenetic analyses of VgRs and related receptors.

MATERIALS AND METHODS

Insects. *Aedes aegypti* were maintained in laboratory culture as described elsewhere (19). Adults were provided with water and a 10% sucrose solution. Vitellogenesis was initiated 3–5 days after eclosion with a blood meal on rats.

Cloning and Sequencing. Purified *Aa*VgR was electroblotted to poly(vinylidene difluoride) (PVDF) membrane (0.2-μm pore size; Bio-Rad) (17) and excised. *Aa*VgR (36 pM, 7.2 μg) was digested with trypsin, the fragments were purified, and N-terminal microsequences were determined for three of these fragments (Harvard Microchem, Cambridge, MA). Degenerate primers based on these microsequences were used in standard PCRs (20) to produce the first *Aa*VgR cDNA fragment (600 bp). It was subcloned into the pBluescript vector (Stratagene) and its identity verified by double-strand sequencing (20, 21) and Northern blot analysis.

Complete sequencing of both strands of two large cDNA fragments making up the entire coding region of the *Aa*VgR was performed in the W. M. Keck facility at Yale University. The deduced amino acid sequence was analyzed with GCG software (University of Wisconsin Genetics Computer Group). Phylogenetic relationships among eight low density lipoprotein receptor (LDLR) superfamily members were calculated (22, 23) using an initial matrix of amino acid identities within a conserved region containing 338 amino acid residues (for details, see figure legends).

mRNA Analyses. Total RNA was extracted and purified from vitellogenic ovarian tissue (18 h after blood meal) by the guanidine isothiocyanate method as described elsewhere (24). Northern blot analyses were performed as described (20). *Aa*VgR cDNA clones were random primer-labeled with ^{32}P and used to probe blots under high-stringency hybridization conditions (21).

***In Situ* Hybridization.** Ovaries were dissected from 3- to 4-day-old previtellogenic mosquitoes and processed for *in situ* hybridization by the method of Suter and Steward (25). A single-strand antisense cDNA probe was prepared by incorporating digoxigenin-11-dUTP into a 600-bp *Aa*VgR cDNA fragment with PCR as described by N. Patel and C. Goodman in the Boehringer Mannheim Applications Manual, and in the Boehringer Mannheim Genius System User's Guide. Sense strands were prepared as controls in the same way. Probe size was reduced by boiling for 1 h in hybridization solution to facilitate tissue penetration. After hybridization, ovaries were incubated with alkaline phosphatase-conjugated anti-digoxigenin antibodies, and the bound complexes were visualized after incubation with nitroblue tetrazolium salt and X-phosphate solution (all from Boehringer Mannheim) for 10–20 min at room temperature. Oocytes were isolated and mounted in Gel/Mount (Biomeda, Foster City, CA).

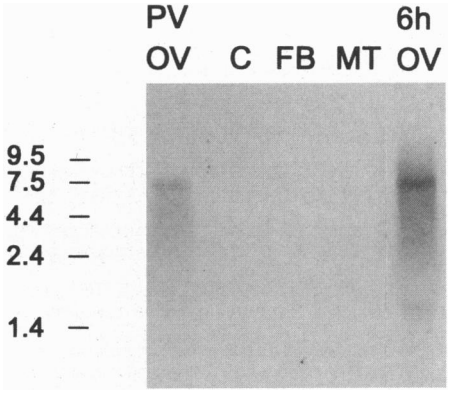

FIG. 1. Northern blot of *Aa*VgR from different tissues. Total RNA (40 μg) extracted from previtellogenic ovaries (PV OV) and vitellogenic female cadavers with ovaries removed (C), fat bodies (FB), and Malpighian tubules (MT) and total RNA (20 μg) from vitellogenic (6 h after a blood meal) ovaries (6 h OV) were separated in a 1.2% agarose/formaldehyde gel. RNA was transferred to nitrocellulose by capillary blotting. The blot was probed with a ^{32}P-labeled 2.7-kb *Aa*VgR cDNA fragment.

RESULTS AND DISCUSSION

Our strategy for determining the primary structure of *Aa*VgR was to obtain short internal amino acid sequences from the purified receptor (17) and design degenerate primers based on these sequences to amplify a larger fragment by PCR and to use the cloned PCR-generated fragment as a probe to screen a vitellogenic-mosquito ovarian cDNA library to isolate full-length or overlapping clones. The N termini of three tryptic fragments yielded high-confidence sequences of 7

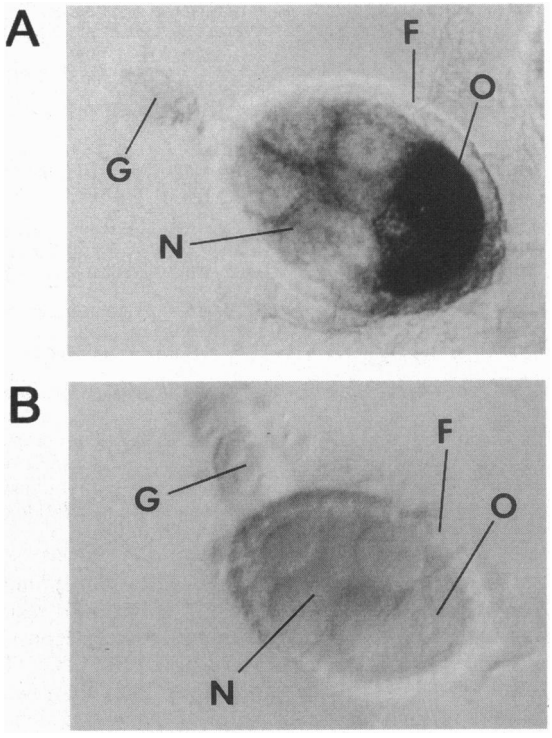

FIG. 2. *In situ* hybridization of *Aa*VgR mRNA in 3- to 4-day-old previtollogenic follicles. Fixed ovaries were incubated with extensively boiled digoxigenin-labeled cDNA probe followed by incubation with alkaline phosphatase-conjugated anti-digoxigenin antibody. *Aa*VgR mRNA was visualized colorimetrically by incubating with nitroblue tetrazolium salt and X-phosphate. (*A*) Follicle probed with antisense cDNA. (*B*) Control follicle probed with sense DNA. O, oocyte; N, nurse cells; F, follicle cells; G, germarium. (×8000.)

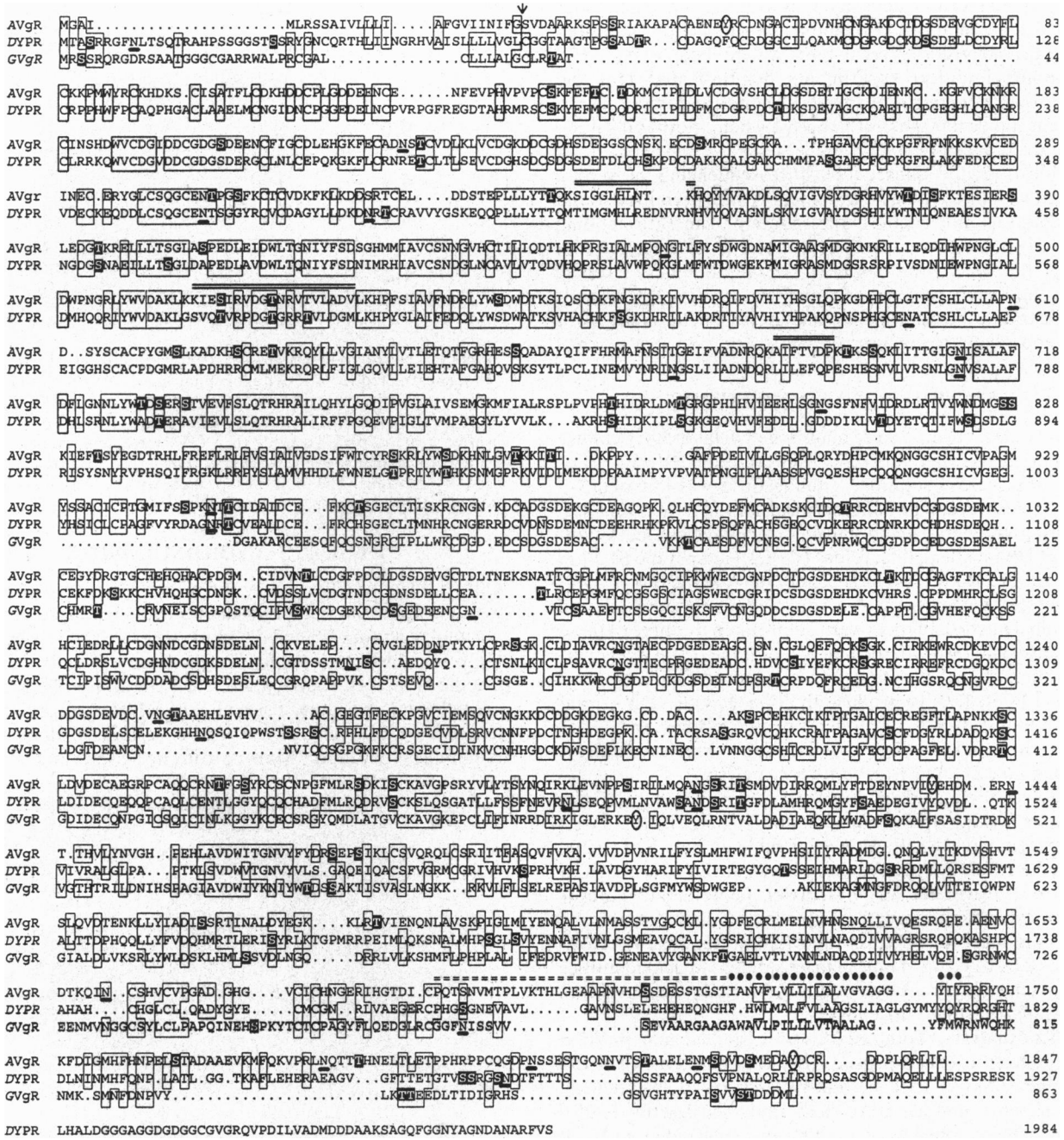

FIG. 3. Deduced amino acid sequence of *Aa*VgR. For comparison, deduced amino acid sequences of *Dm*YPR (15) and *Gg*VgR/LR8 (11) were aligned by the PILEUP program of GCG and adjusted by inspection to align Cys residues. Boxes, identical residues; double overlines, microsequences from tryptic fragments; reverse-phase residues, potential phosphorylation sites; heavy-underlined residues, potential glycosylation sites; circled residues, potential sulfation sites; arrow, putative signal peptide cleavage site; double-dashed overline, *Aa*VgR O-linked sugar domain; solid circles, over *Aa*VgR transmembrane helix.

(AIFTVDP) (TF-1), 10 (SIGGLHLNTK) (TF-2), and 19 (KIESIRVDGTNRVTVLADV) (TF-3) amino acid residues. A degenerate oligonucleotide antisense primer from TF-1 incorporating a *Sph*I restriction site, AAGCATGC(TCAG)AT(TCA)TTT(TC)AC(TCAG)GT(TCAG)GA(TC)CC, and a sense primer designed from the seven 5′-terminal residues of TF-3 incorporating a *Sal*I restriction site, AAGTCGAC(AG)TC(TCAG)GC(TCAG)A(GA)(TCAG)AC(TCAG)GT(TCAG)AC, when used in a PCR amplified a 600-bp cDNA product, which was subcloned into the pBluescript vector (Stratagene). Sequencing demonstrated the presence of both TF-1 and TF-3 sequences at the ends of the 600-bp fragment, including the portion of the TF-3 sequence not used to design the antisense primer.

Confident of its identity as an *Aa*VgR cDNA fragment, we used the 600-bp clone as a probe to screen a λZAPII cDNA library prepared from *A. aegypti* vitellogenic ovaries (gift from R. Graf, University of Zurich, Switzerland). A 2.7-kb clone was isolated and its identity was confirmed by partial sequencing and Northern blot analyses (data not shown). We were unsuccessful in isolating other large overlapping clones from the library, so we employed an alternative strategy. Specific primers were synthesized based on partial sequences from the 2.7-kb clone, and RACE-PCR was performed (26) to the 5′ and 3′ ends of the *Aa*VgR mRNA transcript using, as template, total RNA from ovaries 18 h after the mosquitoes had had a blood meal. 5′-End 2.2-kb and 3′-end 3.2-kb cDNA products were obtained and subcloned into pGEM-5 vectors (Promega).

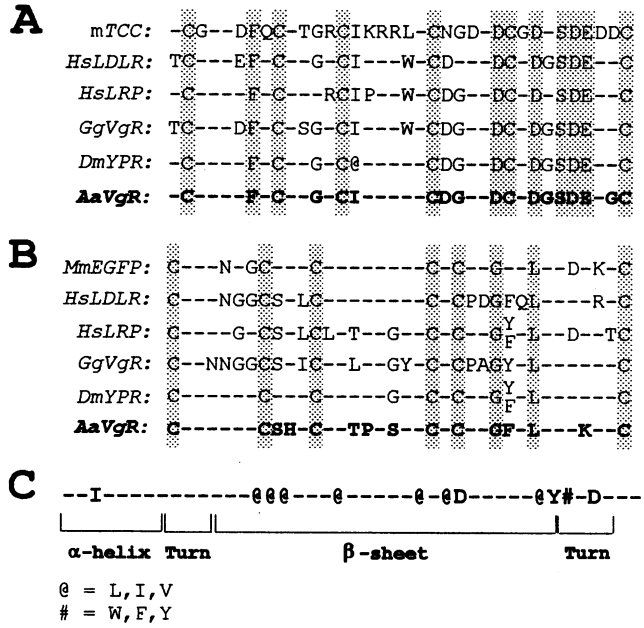

FIG. 4. Consensus sequences for modular repeats characteristic of LDLR superfamily members. Residues common to all consensus sequences are shaded. (*A*) Class A repeats. (*B*) Class B repeats. (*C*) Class C repeat consensus for *Aa*VgR only. Consensus predicted secondary structure is indicated. mTCC, mammalian terminal complement components (i.e., C7–C9) (28); *Hs*LDLR, human LDLR (29); *Hs*LRP, human LDLR-related protein (28); *Mm*EGFP, mouse epidermal growth factor precursor (30).

Identities of the fragments were confirmed by sequencing and Northern blot analyses (data not shown).

Northern blot analyses revealed a single large transcript (≈7.3 kb) restricted to ovarian tissue (Fig. 1). *In situ* hybridization experiments with previtellogenic ovaries indicated that *Aa*VgR mRNA is confined to the oocyte and cytoplasm of nurse cells (Fig. 2). Translation to protein apparently occurs exclusively in the oocyte because previous immunocytochemical studies showed that the protein is not found in the nurse cells (17). Preparation for intensive internalization of massive amounts of *Aa*Vg begins early. Coated-pit and *Aa*VgR accumulation in previtellogenic oocytes begins 1 day after eclosion, reaching levels by day 3 that are maintained until initiation of vitellogenesis by a blood meal (17, 27). *Aa*VgR mRNA was readily detected by *in situ* hybridization in previtellogenic ovaries just 12 h after eclosion and is present even in the germarium containing the secondary oocyte, which will develop only after oviposition of the primary eggs and a second blood meal (data not shown).

The *Aa*VgR amino acid sequence (Fig. 3) was deduced from the overlapping nucleotide sequences of the 2.7-kb and 3.2-kb clones. A Met residue near the beginning of an extended open reading frame was identified within 386 bp of the 5′ end of the 2.7-kb clone, indicating that the entire 2.2-kb 5′-end PCR-generated fragment is part of the 5′-untranslated region. An open reading frame encoding 1847 amino acid residues follows the initial Met. All three partial sequences obtained from microsequencing of tryptic fragments are present in the open reading frame (Fig. 3). The stop codon is succeeded by a polyadenylylation signal (AATAAA) 94 bp downstream, and a poly(A)$^+$ tail 22 bp further downstream.

A putative signal peptide is located at the N-terminus of the pre-*Aa*VgR, and a probable cleavage site is located between residues 26 and 27 (Fig. 3). The predicted molecular mass of the *Aa*VgR after removal of the putative signal peptide is 202.7 kDa, consistent with the estimated molecular masses of 205 kDa for nonreduced and 214 kDa for reduced fully processed *Aa*VgR (17). The predicted isoelectric point of the preprotein is 4.95.

Analyses of the *Aa*VgR deduced amino acid sequence (Fig. 3) indicate that it is a member of the LDLR superfamily. LDLR-type proteins are characterized by a distinctive arrangement of multiple copies of three classes of modular repeats. These include two cysteine-rich motifs each containing six Cys residues: complement-type (class A) (Fig. 4*A*) and epidermal growth factor precursor-type (class B) (Fig. 4*B*). A third type of module, also found in epidermal growth factor, is the ≈43-amino acid YWXD (class C) repeat (Fig. 4*C*).

The modular arrangement of the three classes of repeats in *Aa*VgR is typical of those found in other LDLR-family molecules (Fig. 5). Five to eight class A repeats are arranged tandemly followed by two class B repeats. Clusters of class C repeats are interspersed and flanked by class B repeats. There are 13 complete and 5 partial class C repeats in the *Aa*VgR. Consensus predictions of secondary structure for the *Aa*VgR class C repeats suggest a short two-rotation α-helix and a 27-residue β-sheet separated by four-residue turns (Fig. 4*C*). Between the final extracellular Cys residue (position 1688) and the beginning of the transmembrane domain (position 1723) is a stretch of 34 amino acids rich in Ser and Thr residues (32%), an arrangement conducive to O-linked carbohydrate attachment (31). An O-linked sugar domain in this relative position is common in LDLR-type proteins, but not universal (32). A 22-residue hydrophobic transmembrane helix is followed by a 103-residue cytoplasmic domain (Fig. 3).

There are many possible sites for co- and posttranslational modification (31) of the *Aa*VgR in addition to the O-linked sugar domain, including 16 N-linked glycosylation sites and four tyrosine sulfation sites (Fig. 3). The *Aa*VgR is potentially heavily phosphorylated on Ser and Thr residues, with 64 sites for protein kinase C or casein kinase II and one site for cAMP- or cGMP-dependent protein kinase (position 885) (33). The Asn residues at positions 305 and 1354 may be posttranslationally hydroxylated like the Asn and Asp residues of several

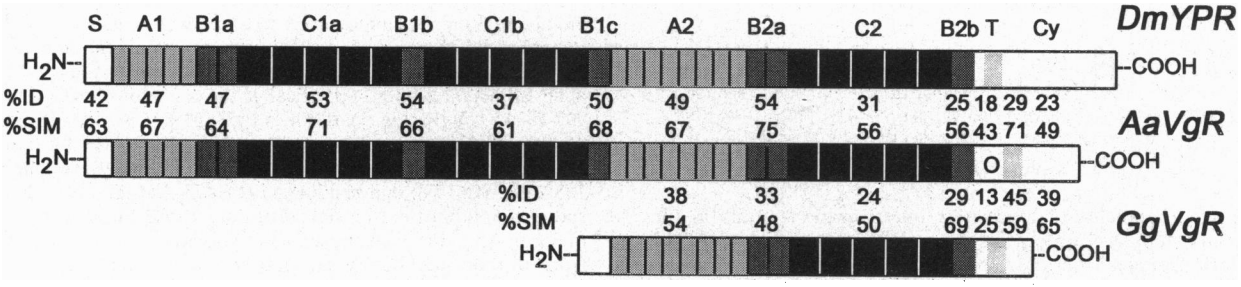

FIG. 5. Schematic alignment of *Aa*VgR modular domains with *Dm*YPR and *Gg*VgR. A, complement-type Cys-rich repeat; B, epidermal growth factor (EGF) precursor-type Cys-rich repeat; C, EGF precursor YWXD-type repeat; T, transmembrane domain; S, signal peptide; O, O-linked sugar domain (*Aa*VgR only); Cy, cytoplasmic tail. Percent identity (%ID) and percent similarity (%SIM) for subdomains were determined by the BESTFIT program of GCG.

other proteins with class B repeats, including human LDLR (34).

The amino acid sequences of the *Gg*VgR/LR8 and *Dm*YPR were recently determined (11, 15), and they also are members of the LDLR superfamily. Although the *Gg*VgR/LR8 is about half the size of the *Aa*VgR and *Dm*YPR, all three show significant similarity in modular arrangement (Fig. 5) and primary structure (Figs. 3 and 4). Percent identities between the *Aa*VgR and the other two receptors are highest in the N-terminal two-thirds of the *Dm*YPR and *Gg*VgR/LR8 (Fig. 5).

The *Aa*VgR differs from both the *Gg*VgR/LR8 and *Dm*YPR in having a putative O-linked sugar domain between the last class B repeat and the transmembrane helix, the consensus position for such regions in LDLR family members. Recently, a splice variant of the *Gg*VgR/LR8 containing a 30-amino acid O-linked sugar domain was identified in somatic tissues (32).

Vertebrate LDLR family members, including the *Gg*VgR/LR8, contain one or more "tight-turn tyrosine" internalization signals (FXNPXY) in the cytoplasmic domain (35). Although the *Aa*VgR and *Dm*YPR share a region of homology with the vertebrate signal, their motifs lack the critical Tyr residue necessary for internalization via clathrin-coated pits (Fig. 6*A*). Instead, both insect receptors contain "di-leucine" (or leucine-isoleucine) motifs (Fig. 6*B*) recently identified as alternative internalization signals in some receptors (35–37).

The striking homology of the *Aa*VgR to the *Dm*YPR (42% amino acid identity and 63% similarity) (Figs. 3 and 5) is very surprising considering the unrelated primary structures of their respective ligands. *Aa*VgR differs from *Dm*YPR in having more potential phosphorylation sites, with only 26% of them in conserved positions (Fig. 3); phosphate moieties are negatively charged and may play a role in ligand recognition. Increasing numbers of vertebrate LDLR superfamily members are being identified as having multiple ligands. For example, the *Gg*VgR/LR8 recognizes at least six different ligands, hence, its recent designation as LR8 (LDLR relative with eight binding repeats) because a ligand-based name is no longer unambiguous (32). LDLR-related proteins (LRP) are very large (300–600 kDa) LDLR superfamily members recognizing multiple ligands. Human LRP and rat gp330 specifically bind and internalize at least 14 (38) and 10 (39) different ligands, respectively, including lipoprotein lipase, the family to which *Drosophila*-like YPs belong. In the chicken, two species of LRP bind and internalize *Gg*Vg among other ligands (40). It is possible that we will find, on closer examination, that *ins*VgRs and YPRs internalize more than one yolk-protein precursor like their vertebrate counterparts. Ligand competition experiments suggest that Vg and high-density lipophorin are internalized by a single receptor in the oocytes of a moth, *Hyalophora cecropia* (41).

Little is known about insect lipoprotein lipases apart from the species found in locust flight muscle (42). However, lipoprotein lipase has been detected in the yolk of *Manduca sexta* eggs (43). Its source is unknown, but given the putative affinity of *Dm*YPR for a lipoprotein lipase-related protein and of vertebrate LRPs for lipoprotein lipases, it seems distinctly possible that *ins*VgRs internalize this enzyme in addition to Vg. *A. aegypti* oocytes internalize at least two additional extraovarially sythesized yolk-protein precursors during vitellogenesis for storage in yolk bodies (19, 44), but their receptor(s) are as yet unidentified.

*Aa*VgR and *Dm*YPR are no more similar to *Gg*VgR/LR8 (32% and 29% amino acid identity, respectively) than to other members of the vertebrate LDLR superfamily (range of 27–32% identity). Proposed phylogentic relationships among LDLR superfamily members based on amino acid distances (Fig. 7) and parsimony analyses (data not shown) suggest that both the *ins*VgR/YPR lineage and the vertebrate VgR/LDLR lineage are more ancient than the divergence between the nematode and deuterostome lines. As a corollary, it suggests that the original LDLR superfamily progenitor arose in an acoelomate. This ancestral molecule may have been a large LRP-like receptor from which smaller LDLR superfamily members are derived (15). Alternatively, it has been hypothesized (13) that LR8-type receptors such as *Gg*VgR/LR8 may represent a primordial multifunctional yolk-protein precursor receptor from which more specialized receptors, such as LDLRs and LRPs, are derived. Our phylogenetic analysis points to a third prospect that must now be considered, namely, that the intermediate-sized *ins*VgR/YPR class receptors represent the primordial type from which larger and smaller receptors are derived. We predict that LDLR superfamily members will be identified in organisms more primitive than nematodes and that their characterization will elucidate the evolutionary origins of this fascinating and physiologically important class of protein.

Finally, the proposed phylogeny (Fig. 7) presents an interesting paradox with regard to the coevolution of receptor–ligand interactions. Two receptors (*Aa*VgR and *Dm*YPR) related by relatively recent common ancestry specifically recognize unrelated ligands (*Aa*Vg and *Dm*YPs), while two receptors (*Aa*VgR and *Gg*VgR/LR8) from lineages sharing

A

*Hs*LDLR	11	INFDNPVY
*Hs*LRP	56	TNFTNPVY
*Gg*VgR	11	MNFDNPVY
*Dm*YPR	12	MHFQNPLA
AaVgR	12	MHFHNPEL

B

TCR	128	QTLL
gp130	143	QPLL
*Dm*YPR	76	QRLL
*Dm*YPR	92	QELL
AaVgR	98	QRLI

FIG. 6. Alignments of alternative internalization motifs in the cytoplasmic domains of receptors. Numerals indicate the number of amino acid residues from the C-terminal end of the transmembrane domain of each receptor. (*A*) Tight-turn tyrosine motif. Underline, tyrosine residue necessary for internalization. (*B*) Di-leucine (or leucine-isoleucine) motif. TCR, T-cell antigen receptor (36); gp130, interleukin 6 signal transducer (37). Other abbreviations are as in Fig. 4.

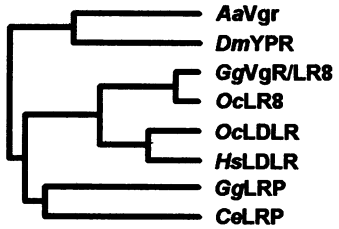

FIG. 7. Phylogenetic relationships among eight LDLR superfamily members. Regions homologous to the seven class A and the two immediately following class B Cys-rich repeats of the human LDLR were aligned with the PILEUP program of GCG and adjusted by eye to align all Cys residues. Specifically, these regions include residues 997-1371, *Aa*VgR (Fig. 3); residues 1053–1435, *Dm*YPR (15); residues 46–408, *Gg*VgR/LR8 (11); residues 45–407, *Oc*LR8 (45); residues 6–371, *Oc*LDLR (46); residues 27–392, *Hs*LDLR (29); residues 1316–1682, *Gg*LRP (47); and residues 1101–1475, *Ce*LRP (48). This corresponds to all but the first repeat of domain A2 through domain B2a of Fig. 5. Areas in which any sequence contained a gap were eliminated from all sequences before calculation of amino acid identities. Thus, the final number of residues compared was 338. Lengths of branches along the horizontal axis are proportional to evolutionary distances calculated from the amino acid identity matrix. *Ce*, *Caenorhabditis elegans* (nematode); *Oc*, *Oryctolagus cuniculus* (rabbit). Other abbreviations are as in Fig. 4.

only a very distant common ancestor recognize related ligands (*Aa*Vg and *Gg*Vg).

We thank Avraham Biran, Marina Kapitskaya, Neal Dittmer, Shengfu Wang, and Alan Hays for critical reading of the manuscript and for many helpful suggestions. This research was supported by a grant (AI-32154) from the National Institutes of Health to A.S.R.

1. Goldstein, J. L., Anderson, R. G. W. & Brown, M. S. (1979) *Nature (London)* **279,** 679–685.
2. Bu, G. & Schwartz, A. L. (1994) in *The Liver: Biology and Pathology*, eds. Arias, I. M., Boyer, J. L., Fausto, N., Jakoby, W. B., Schachter, D. A. & Shafritz, D. A. (Raven, New York), pp. 259–274.
3. Koller, C. N., Dhadialla, T. S. & Raikhel, A. S. (1989) *Insect Biochem.* **19,** 693–702.
4. Sauer, J. R., McSwain, J. L. & Essenberg, R. C. (1994) *Int. J. Parisitol.* **24,** 33–52.
5. Chen, J.-S., Cho, W. -L. & Raikhel, A. S. (1994) *J. Mol. Biol.* **237,** 641–647.
6. Raikhel, A. S. & Dhadialla, T. S. (1992) *Annu. Rev. Entomol.* **37,** 217–251.
7. Schneider, W. J. (1995) *Curr. Opin. Lipidol.* **6,** 92–96.
8. Sappington, T. W. & Raikhel, A. S. (1995) in *Recent Advances in Insect Biochemistry and Molecular Biology*, ed. Takahashi, S. (Nagoya Univ. Press, Nagoya, Japan), pp. 235–257.
9. Speith, J. & Blumenthal, T. (1985) *Mol. Cell Biol.* **5,** 2495–2501.
10. Wahli, W. (1988) *Trends Genet.* **4,** 227–232.8.
11. Bujo, H., Hermann, M., Kaderli, M. O., Jacobsen, L., Sugawara, S., Nimpf, J., Yamamoto, T. & Schneider, W. J. (1994) *EMBO J.* **13,** 5165–5175.
12. Jacobsen, L., Hermann, M., Vieira, P. M., Schneider, W. J. & Nimpf, J. (1995) *J. Biol. Chem.* **270,** 6468–6475.
13. Hiesberger, T., Hermann, M., Jacobsen, L., Novak, S., Hodits, R. A., Bujo, H., Meilinger, M., Huttinger, M., Schneider, W. J. & Nimpf, J. (1995) *J. Biol. Chem.* **270,** 18219–18226.
14. Bownes, M., Shirras, A., Blair, M., Collins, J. & Coulson, A. (1988) *Proc. Natl. Acad. Sci. USA* **85,** 1554–1557.
15. Schonbaum, C. P., Lee, S. & Mahowald, A. P. (1995) *Proc. Natl. Acad. Sci. USA* **92,** 1485–1489.
16. Ferenz, H.-J. (1993) *Int. J. Insect Morphol. Embryol.* **22,** 295–314.
17. Sappington, T. W., Hays, A. R. & Raikhel, A. S. (1995) *Insect Biochem. Mol. Biol.* **25,** 807–817.
18. Dhadialla, T. S., Hays, A. R. & Raikhel, A. S. (1992) *Insect Biochem. Mol. Biol.* **22,** 803–816.
19. Hays, A. R. & Raikhel, A. S. (1990) *Roux's Arch. Devel. Biol.* **199,** 114–121.
20. Cho, W.-L. & Raikhel, A. S. (1992) *J. Biol. Chem.* **267,** 21823–21829.
21. Sambrook, J., Fritsch, E. & Maniatis, T. (1989) *Molecular Cloning: A Laboratory Manual* (Cold Spring Harbor Lab. Press, Plainview, NY), 2nd Ed.
22. Kimura, M. (1983) *The Neutral Theory of Molecular Evolution* (Cambridge Univ. Press, Cambridge, U.K.).
23. Swofford, D. L. & Olsen, G. J. (1990) in *Molecular Systematics*, eds. Hillis, D. M. & Moritz, C. (Sinauer, Sunderland, MA), Chap. 11.
24. Bose, S. G. & Raikhel, A. S. (1988) *Biochem. Biophys. Res. Commun.* **155,** 436–442.
25. Suter, B. & Steward, R. (1991) *Cell* **67,** 917–926.
26. Frohman, M. A., Dush, M. K. & Martin, G. R. (1988) *Proc. Natl. Acad. Sci. USA* **85,** 8998–9002.
27. Raikhel, A. S. & Lea, A. O. (1985) *Gen. Comp. Endocrinol.* **53,** 424–435.
28. Herz, J., Hamann, U., Rogne, S., Myklebost, O., Gausepohl, H. & Stanley, K. K. (1988) *EMBO J.* **7,** 4119–4127.
29. Yamamoto, T., Davis, C. G., Brown, M. S., Schneider, W. J., Casey, M. L., Goldstein, J. L. & Russel, D. W. (1984) *Cell* **39,** 27–38.
30. Gray, A., Dull, T. J. & Ullrich, A. (1983) *Nature (London)* **303,** 722–725.
31. Creighton, T. E. (1993) *Proteins* (Freeman, New York).
32. Bujo, H., Yamamoto, T., Hayashi, K., Hermann, M., Nimpf, J. & Schneider, W. J. (1995) *Proc. Natl. Acad. Sci. USA* **92,** 9905–9909.
33. Kemp, B. E. & Pearson, R. B. (1990) *Trends Biochem. Sci.* **15,** 342–346.
34. Stenflo, J., Ohlin, A.-K., Owens, W. G. & Schneider, W. J. (1988) *J. Biol. Chem.* **263,** 21–24.
35. Trowbridge, I. S., Collawn, J. F. & Hopkins, C. R. (1993) *Annu. Rev. Cell Biol.* **9,** 129–161.
36. Letourneur, F. & Klausner, R. D. (1992) *Cell* **69,** 1143–1157.
37. Dittrich, E., Rose-John, S., Gerhartz, C., Mullberg, J., Stoyan, T., Yasukawa, K., Heinrich, P. C. & Graeve, L. (1994) *J. Biol. Chem.* **269,** 19014–19020.
38. Williams, S. E., Kounnas, M. Z., Argraves, K. M., Argraves, W. S. & Strickland, D. K. (1994) *Ann. N.Y. Acad. Sci.* **737,** 1–13.
39. Kounnas, M. Z., Stefansson, S., Loukinova, E., Argraves, K. M., Strickland, D. K. & Argraves, W. S. (1994) *Ann. N.Y. Acad. Sci.* **737,** 114–123.
40. Nimpf, J. & Schneider, W. J. (1994) *Ann. N.Y. Acad. Sci.* **737,** 145–153.
41. Kulakosky, P. C. & Telfer, W. H. (1990) *Arch. Insect Biochem. Physiol.* **14,** 269–285.
42. van Heusden, M. C., van der Horst, D. J., van Doorn, J. M. & Beenakkers, A. M. T. (1987) *Comp. Biochem. Physiol. [B]* **88,** 523–527.
43. van Antwerpen, R. & Law, J. H. (1992) *Arch. Insect Biochem. Physiol.* **20,** 1–12.
44. Cho, W.-L., Deitsch, K. W. & Raikhel, A. S. (1991) *Proc. Natl. Acad. Sci. USA* **88,** 10821–10824.
45. Takahashi, S., Kawarabayasi, Y., Nakai, T., Sakai, J. & Yamamoto, T. (1992) *Proc. Nat. Acad. Sci. USA* **89,** 9252–9256.
46. Yamamoto, T., Bishop, R. W., Brown, M. S., Goldstein, J. L. & Russel, D. W. (1986) *Science* **232,** 1230–1237.
47. Nimpf, J., Stifani, S., Bilous, P. T. & Schneider, W. J. (1994) *J. Biol. Chem.* **269,** 212–219.
48. Yochem, J. & Greenwald, I. (1993) *Proc. Natl. Acad. Sci. USA* **90,** 4572–4576.